SPANDIDOS PUBLICATIONS

Pre-clinical evaluation of [^{111}In]-benzyl-DOTA-$Z_{HER2:342}$, a potential agent for imaging of HER2 expression in malignant tumors

ANNA ORLOVA[1,2], THUY TRAN[1], CHARLES WIDSTRÖM[3], TORUN ENGFELDT[4], AMELIE ERIKSSON KARLSTRÖM[4] and VLADIMIR TOLMACHEV[1,2,5]

[1]Unit of Biomedical Radiation Sciences, Rudbeck Laboratory, Uppsala University, Uppsala; [2]Affibody AB, Bromma; [3]Section of Hospital Physics, Department of Oncology, Uppsala University Hospital, Uppsala; [4]School of Biotechnology, Royal Institute of Technology, Stockholm; [5]Department of Medical Sciences, Nuclear Medicine, Uppsala University, Uppsala, Sweden

Received March 29, 2007; Accepted May 3, 2007

Abstract. Imaging of expression of human epidermal growth factor receptor type 2 (HER2) in breast carcinomas may help to select patients eligible for trastuzumab therapy. The Affibody molecule $Z_{HER2:342}$ is a small (7-kDa) non-immunoglobulin affinity protein, which binds to HER2 with a picomolar affinity. Previously, a benzyl-DTPA conjugate of $Z_{HER2:342}$ was labeled with ^{111}In and demonstrated good targeting in murine xenografts. We considered that the use of the macrocyclic chelator DOTA could increase the label stability and enhance a choice of nuclides, which could be used as a label for $Z_{HER2:342}$. The goal of this study was the preparation and pre-clinical evaluation of the indium-111-labeled DOTA-derivative of $Z_{HER2:342}$. Isothiocyanate-benzyl-DOTA was coupled to recombinant $Z_{HER2:342}$, and the conjugate was efficiently labeled with ^{111}In at 60˚C. The specificity of ^{111}In-benzyl-DOTA-$Z_{HER2:342}$ binding to HER2 was confirmed *in vitro* using HER2-expressing breast carcinoma BT474 and ovarian carcinoma SKOV-3 cell lines. Biodistribution of ^{111}In-benzyl-DOTA-$Z_{HER2:342}$ was performed in nude mice bearing LS174T xenografts and compared directly with the biodistribution of ^{111}In-benzyl-DTPA-$Z_{HER2:342}$. *In vivo*, ^{111}In-benzyl-DOTA-$Z_{HER2:342}$ demonstrated quick clearance from blood and non-specific organs except the kidneys. Four hours post injection (pi), the tumor uptake of ^{111}In-benzyl-DOTA-$Z_{HER2:342}$ (4.4±1.0% IA/g) was specific and the tumor-to-blood ratio was 23. The use of benzyl-DTPA provided higher tumor-to-blood and tumor-to-liver ratios. γ-camera imaging showed clear visualization of HER2-expressing xenografts using ^{111}In-benzyl-DOTA-$Z_{HER2:342}$. ^{111}In-benzyl-DOTA-$Z_{HER2:342}$ has a potential for imaging of HER2 expression in malignant tumors.

Correspondence to: Dr Vladimir Tolmachev, Division of Biomedical Radiation Sciences, Rudbeck Laboratory, Uppsala University, S-751 85 Uppsala, Sweden
E-mail: vladimir.tolmachev@bms.uu.se

Key words: Affibody, human epidermal growth factor receptor type 2, tumor targeting, indium-111, benzyl-DOTA

Introduction

Progress in tumor biology has helped to identify a number of receptors, the aberrant expression of which is essential for malignant transformation. Mitogenic signaling of these receptors makes it possible for the tumors to escape proliferation control. One of these receptors is the human epidermal growth factor receptor type 2 (HER2), a member of the transmembrane tyrosine kinase receptor family. According to the contemporary paradigm, HER2 is an orphan receptor which has no ligand. Signaling occurs by heterodimerisation with other receptors, especially HER3, and increases the mitotic signal of these receptors (1). HER2 is not expressed in normal tissues, or its expression is low. Among malignant tumors, expression of HER2 was detected in 25-30% of breast and ovarian carcinomas (2,3) and in 80% of bladder carcinomas (4). The disruption of signaling of HER2 is considered as a promising way of treating malignant tumors. Such strategies include the use of monoclonal antibodies, for example trastuzumab (5) and pertuzumab (6) or degradation of HER2 expression (7). The humanized monoclonal antibody trastuzumab has confirmed clinical efficacy for treatment of breast cancer and has been accepted for routine clinical use (8). Apparently, such therapy can be efficiently used only for patients with tumors expressing HER2. For this reason, determining the HER2 status in each case of breast cancer is recommended both in the US and in Europe (9,10). Detection of HER2 status might be helpful also for the monitoring of anti-HER2 therapy (11). Taking into account that biopsy samples can produce false-negative results, and that the metastases of HER2-negative tumors can express HER2 (12), a development of efficient radionuclide methods for visualization of HER2 expression *in vivo* is desirable.

Earlier approaches to use nuclear medicine for detection of HER2 expression for selection of patients eligible for trastuzumab treatment have been associated with the use of radiolabeled trastuzumab. Behr and co-workers (13) demonstrated that ^{111}In-labeled trastuzumab can help to select patients responding to antibody treatment, as well as predict cardiotoxicity. However, a later study (14) showed that only 45% of the tumors were detected by ^{111}In-trastuzumab. The lack of sensitivity could be explained by the low contrast, which is typical for intact immunoglobulins, characterized by slow tumor penetration and slow blood clearance. Size reduction of tumor-targeting proteins improves these parameters, and radiolabeled $(Fab')_2$ (11,15), Fab (16) and single-chain Fv (17) fragments of trastuzumab have been obtained and pre-clinically evaluated to improve contrast and facilitate imaging. Further size reduction can be achieved by the use of non-immunoglobulin scaffold-based affinity proteins, which are selected by phage, cell surface or ribosomal display (18), such as Affibody molecules.

Affibody molecules (19) use the domain scaffold of the immunoglobulin-binding staphylococcal protein A. This 58-amino-acid-long cysteine-free protein provides a robust framework, independent of disulfide bonds for its folding. The small size (~7 kDa in the monomeric and ~15 kDa in the dimeric form) of Affibody molecules enables fast blood clearance and good tumor penetration. Randomization of 13 solvent-accessible surface residues of the protein A domain was used to create a library containing about $3x10^9$ members, providing the isolation of high-affinity ligands for virtually any tumor-associated protein target. Phage display was used to select an anti-HER2 Affibody molecule $Z_{HER2:4}$, which binds HER2 with an affinity of 50 nM (20,21). We have found that the indirectly radioiodinated and radiobrominated dimeric form of $Z_{HER2:4}$ (affinity of 3 nM) can specifically target HER2-expressing xenografts, providing a tumor-to-blood ratio between 2 and 9 at 4 h pi, depending on the labeling methods and the number of prosthetic groups per protein molecule (22-24). Affinity maturation of $Z_{HER2:4}$ provided a new clone, $Z_{HER2:342}$, with an affinity of 22 pM (25). Indirect radioiodination of $Z_{HER2:342}$ resulted in a tracer with a tumor-to-blood ratio of 37 for SKOV-3 xenografts in mice 4 h pi (25).

Though ^{123}I possesses excellent imaging and dosimetric properties, indirect radioiodination requires well-trained personnel, and the short half-life of ^{123}I complicates the logistics. To facilitate clinical implementation of the $Z_{HER2:342}$ Affibody molecule, we developed a procedure for ^{111}In labeling of $Z_{HER2:342}$ conjugated with benzyl-DTPA via a thiourea bond (26). The use of benzyl-DTPA as a chelator ensured facile labeling permitting kit formulation and provided a tumor-to-blood ratio of 94 in SKOV-3 xenografts 4 h pi.

The selection of a labeling method is always a trade-off between several requirements. We used benzyl-DTPA in a previous study because of the easy and quick labeling at room temperature. Some publications (27,28) suggest that the use of DOTA derivatives requires heating up to 100˚C for efficient indium labeling, and that labeling at lower temperatures is rather inefficient (29). On the other hand, the gallium-DTPA complex is not considered to be sufficiently stable *in vivo* (30), and the use of PET with ^{68}Ga-labeled $Z_{HER2:342}$ for visualization of HER2 would require the use of a macrocyclic chelator. The robust structure of Affibody molecules and quick and accurate refolding after denaturation give an opportunity to use elevated temperatures for labeling. For this reason, we evaluated the labeling of the anti-HER2 $Z_{HER2:342}$ Affibody molecule using isothiocyanate-benzyl-DOTA. Since different chelators may have a profound influence on the biodistribution of labeled peptides (31), *in vivo* tumor targeting using ^{111}In-benzyl-DTPA- $Z_{HER2:342}$ and ^{111}In-benzyl-DOTA-$Z_{HER2:342}$ was directly compared in this study.

Materials and methods

The Affibody molecule $Z_{HER2:342}$ was produced according to Orlova *et al* (26), and was provided for this study by Affibody AB (Bromma, Sweden) as a 2.22-mg/ml solution in PBS. Isothiocyanate-benzyl-DOTA was purchased from Macrocyclics (Dallas, TX, USA), and [^{111}In]indium chloride from Tyco Healthcare Norden AB (Sweden). Buffers were prepared using common methods from chemicals supplied by Merck (Darmstadt, Germany). Buffers for conjugation and labeling were purified from metal contamination using Chelex 100 resin (Bio-Rad Laboratories, Richmond, CA, USA). The NAP-5 size exclusion columns were from Amersham Biosciences (Uppsala, Sweden). The ^{111}In-benzyl-DTPA-$Z_{HER2:342}$ conjugate for the comparative biodistribution experiment was prepared according to the procedure described by Tolmachev *et al* (26).

The radioactivity was measured using an automated γ-counter with a 3-inch NaI(Tl) detector (1480 Wizard, Wallac Oy, Turku, Finland). The distribution of radioactivity along the ITLC SG (silica gel impregnated glass fiber sheets for instant thin layer chromatography, Gelman Sciences Inc.) strips was measured on the Cyclone™ Storage Phosphor system and analyzed using the OptiQuant™ image analysis software.

Conjugation and labeling chemistry. The conjugation of isothiocyanate-benzyl-DOTA to the Affibody molecule $Z_{HER2:342}$ was performed similarly to the method described by Tolmachev *et al* (26), using a calculated chelator-to-protein molar ratio of 1:1, 2:1 or 3:1. Briefly, 500 μg of $Z_{HER2:342}$ was mixed with freshly prepared solution of isothiocyanate-benzyl-DOTA in 0.07 M sodium borate buffer, pH 9.2. The mixture was incubated overnight at 37˚C. The reaction mixture was purified on a NAP-5 size exclusion column with 1 M ammonium acetate buffer, pH 5.5.

The DOTA-coupling efficiency was evaluated by running analytical RP-HPLC of benzyl-DOTA-$Z_{HER2:342}$, using a 4.5x150-mm column with a polystyrene/divinylbenzene matrix of 5-μm particles (Amersham Biosciences) at a flow of 1 ml/min and a 20-min elution gradient of 20-50% B (A, 0.1% TFA-H_2O; B, 0.1% TFA-CH_3CN). The molecular weights were confirmed by MALDI-TOF-MS.

Real-time biospecific interaction analysis was performed on a Biacore 2000 instrument (Biacore, Uppsala, Sweden) to measure the binding kinetics of the benzyl-DOTA-$Z_{HER2:342}$.

cellular domain of HER2 (from Professor Gregory Fox Chase Cancer Center, Philadelphia, PA, USA) and human serum albumin, HSA, (Kabi Vitrum, Stockholm, Sweden) were diluted to 20 μg/ml in 10 mM NaOAc, pH 4.5 and immobilized on a CM5 sensor chip (Biacore, Uppsala, Sweden). The samples were diluted in the running buffer HBS (10 mM HEPES, 150 mM NaCl, 3.4 mM EDTA and 0.005% Surfactant P20, pH 7.4) to 0.3-20 nM and injected at a flow rate of 50 μl/min. HCl (20 mM) was used for surface regeneration.

The labeling was performed at 60˚C. To study the labeling kinetics, a 40-μg conjugate was mixed with 40 MBq ^{111}In and incubated for 60 min. The experiment was performed in triplicate. At pre-determined points of time (5, 15, 30 and 60 min), a sample of 0.5 μl was taken and analyzed using ITLC with 0.2 M citric acid.

When the labeling procedure was established, a 15-min-long labeling was used. In some cases, e.g. for biodistribution experiments, the buffer was exchanged by sterile PBS using a NAP-5 column. For cell studies, the reaction mixture was diluted with PBS.

For a label stability test, two samples of benzyl-DOTA-$Z_{HER2:342}$ were labeled with ^{111}In and 5-μl samples were mixed either with 62 μl of PBS or with 62 μl of sodium salt of EDTA (20 mg/ml in PBS, 10,000-fold molar excess). The samples were incubated at room temperature. At pre-determined points of time, 1, 3 and 24 h, the samples were analyzed using ITLC.

Cell binding and retention studies. The HER2-expressing ovarian carcinoma cell line SKOV-3 and the breast carcinoma cell line BT474 (both from ATCC) were used for the binding specificity test. A labeled conjugate (7 ng) was added to two groups of three Petri dishes (5x10^5 cells per dish). One group of dishes in each experiment was pre-saturated with a 1,000-fold excess of non-labeled Affibody. The cells were incubated with labeled conjugate for 1 h at 37˚C, and the incubation media was collected. The cell dishes were washed and treated with 0.5 ml trypsin-EDTA solution (0.25% trypsin, 0.02% EDTA in buffer; Flow Irvine, UK). When the cells were detached, 0.5 ml complete medium was added to each dish, and the cells were re-suspended for radioactivity measurement.

The cellular retention of radioactivity after interrupted incubation was studied according to Tolmachev *et al* (26). Briefly, culture dishes were incubated for 2 h with culture medium containing 7 ng ^{111}In-benzyl-DOTA-$Z_{HER2:342}$. The dishes were then washed and incubated at 37˚C with fresh complete media. At pre-determined points of time the incubation media was collected from the 3 culture dishes, and the cells were detached from the culture dishes by trypsin treatment, as described above. The radioactivity associated with the cells and the culture media was measured. The fraction of the initial cell-associated radioactivity was analyzed as a function of time.

Biodistribution studies. The animal studies were approved by the local Ethics Committee for Animal Research. In all the biodistribution studies, the mice were euthanized with an intraperitoneal injection of Ketalar-Rompun solution. The mice were exsanguinated by heart puncture. Blood and organ samples were collected and weighed, and their radioactivity was recorded using an automatic γ-counter. To evaluate the degree of hepatobiliary excretion, the radioactivity in the entire gastrointestinal tract with its content was measured and expressed as % IA per whole sample. The radioactivity in the carcass was evaluated as well and presented as % IA per whole sample. Tissue uptake values were calculated as percent of injected activity per gram tissue (% IA/g).

Biodistribution in immunocompetent NMRI mice was performed on 12 mice that were sc injected with 50 kBq ^{111}In-benzyl-DOTA-$Z_{HER2:342}$ (protein dose 1 μg). At 1, 4 and 24 h pi, a group of 4 animals was euthanized and dissected.

The LS174T cell line was used in biodistribution experiments on tumor-bearing mice. According to Milenic and co-authors (32,33), this cell line possesses low but uniform expression of HER2 and may be a good model to demonstrate the sensitivity of $Z_{HER2:342}$ in detection of low-level antigen expression. Female outbred Balb/c nu/nu mice were sc injected with one million LS174T cells in the hind leg 3 weeks before the experiment.

Twelve Balb/c nu/nu mice with LS174T xenografts were randomly divided into 3 groups of 4 animals each. One group was sc injected in the neck area with 475 μg of non-labeled $Z_{HER2:342}$ in PBS. One hour later, 2 groups of mice (1 blocked and 1 non-blocked) were sc injected with ^{111}In-benzyl-DOTA-$Z_{HER2:342}$ at a protein dose of 1 μg (~100 kBq) in 100 μl PBS. Additionally, 1 group of mice was injected with the same amount of ^{111}In-benzyl-DTPA-$Z_{HER2:342}$ to compare the tumor-targeting properties of the conjugates. At 4 h pi the mice were euthanized and dissected.

γ-camera imaging. Female outbred Balb/c nu/nu mice were sc injected with 10^7 SKOV-3 cells in the hind leg 8 weeks before the experiment. At the time of the imaging, the tumors were ~0.5-0.8 cm^3. Two animals were injected with 3 MBq (5 μg) ^{111}In-benzyl-DOTA-$Z_{HER2:342}$ in the tail vein. The imaging was performed 4 h pi using a Siemens e.CAM γ-camera (Siemens Medical Systems) equipped with an MEGP collimator at the Department of Nuclear Medicine, Uppsala University Hospital. Static images (10 min, 550,000 counts), obtained with a zoom factor of 3.2, were digitally stored in a 256x256 matrix. The pixel size was 2.4 mm. The scintigraphic results were evaluated visually and analyzed quantitatively using Hermes software (Nuclear Diagnostics, Stockholm, Sweden). The quantitative analysis was performed by drawing equal regions of interest (ROI) over the tumor and contralateral thigh, as well as ROI over the kidneys and upper abdomen (liver). Tumor-to-non-tumor ratios were calculated based on counts per pixel.

Results

Conjugation and labeling chemistry. Data of the LC-MS analysis suggested that a single chelator was attached to 59% of the protein molecules, while 15% of the protein remained unconjugated when a 3:1 chelator to protein ratio was used for coupling. Biospecific interaction analysis showed that the binding affinity was somewhat reduced in comparison with non-conjugated $Z_{HER2:342}$ but still in the subnanomolar range.

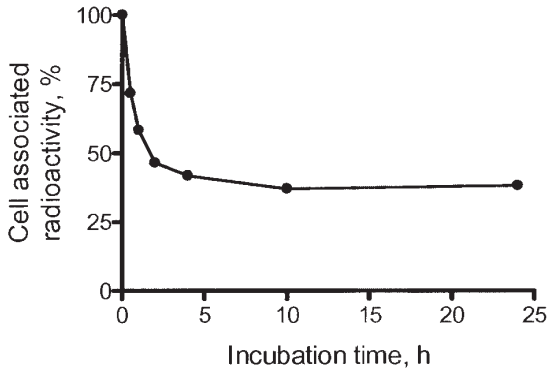

Figure 1. Cell-associated ^{111}In radioactivity as a function of time after interrupted incubation of SKOV-3 cells with ^{111}In-benzyl-DTPA-$Z_{HER2:342}$. The cell-associated radioactivity at time zero after the interrupted incubation was considered as 100%. Data are the mean ± SD (n=3). Error bars might not be seen because they are smaller than point symbols.

The labeling kinetics was fast; even a 5-min-long reaction at 60˚C provided a labeling yield of >97%, with only a minor increase when the labeling was prolonged up to 60 min.

The radiolabeled conjugate retained its stability in PBS for at least 3 h (95.7±0.2% of ^{111}In associated with Affibody conjugate at a 3-h and 94±1% at a 24-h incubation). The stability at a large molar excess of EDTA confirmed that ^{111}In was attached via a stable DOTA chelate and not by an occasional combination of amino acids with weak chelating capacity (95.05±0.05 and 89.6±0.4% at a 3- and 24-h incubation, respectively).

Cell binding and retention studies. The specificity of ^{111}In-benzyl-DOTA-$Z_{HER2:342}$ binding to living HER2-expressing cells was controlled using the ovarian carcinoma cell line SKOV-3 and the breast carcinoma cell line BT474. The addition of a large excess of non-labeled $Z_{HER2:342}$ caused a substantial, 50- to 80-fold decrease in the attachment of radioactivity to cells in both cell lines (18±1 vs. 0.4±0.1% added radioactivity associated with cells for BT474 and 9.0±0.6 vs. 0.11±0.08% for SKOV-3, $p<0.0001$). This showed the saturable nature of ^{111}In-benzyl-DOTA-$Z_{HER2:342}$ binding and indicated that the binding was receptor specific.

The retention pattern of ^{111}In radioactivity after the interrupted incubation of ^{111}In-benzyl-DOTA-$Z_{HER2:342}$ with SKOV-3 is shown in Fig. 1. Generally, it is similar to the curve obtained previously for ^{111}In-benzyl-DTPA-$Z_{HER2:342}$ (26). The curve is characterized by two segments. An initial drop of radioactivity during the first 4 h after interrupted incubation was followed by a relatively constant amount of cell-associated ^{111}In. This curve shape might be explained in the following way. Internalization of bound ^{111}In-benzyl-DOTA-$Z_{HER2:342}$ seems to be relatively slow, and, after change of culture medium, a substantial part of the conjugate was dissociated in non-degraded form. At the same time, a part of the conjugate was internalized, and this made the cell association of radioactivity practically irreversible due to the residualizing properties of the ^{111}In label. Note that the level of the plateau is lower for ^{111}In-benzyl-DOTA-$Z_{HER2:342}$ (38-40%) than was reported for ^{111}In-benzyl-DTPA-$Z_{HER2:342}$ (46-52%), which correlates well with the lower affinity of ^{111}In-benzyl-DOTA-$Z_{HER2:342}$. An internalization assay could be helpful towards a more accurate interpretation. However, as we pointed out previously (26) part of labeled $Z_{HER2:342}$, independently of the label, always binds to HER2-expressing cells irreversibly, and can be removed neither by acid wash nor by displacement by a large excess of non-labeled $Z_{HER2:342}$.

Table I. Biodistribution of ^{111}In-benzyl-DOTA-$Z_{HER2:342}$ in normal NMRI mice.[a]

	Radioactivity concentration in organs, % IA/g		
	1 h	4 h	24 h
Blood	1.1±0.2	0.21±0.04	0.11±0.02
Heart	0.45±0.04	0.17±0.02	0.14±0.01
Lung	1.0±0.1	0.41±0.06	0.28±0.06
Liver	1.3±0.2	1.6±0.3	1.3±0.2
Spleen	0.53±0.08	0.4±0.1	0.44±0.07
Colon[b]	0.8±0.2	0.6±0.1	0.41±0.08
Kidney	146±31	177±16	124±14
Skin	0.7±0.1	0.3±0.1	0.19±0.06
Muscle	0.18±0.08	0.07±0.02	0.06±0.01
Bone	0.4±0.1	0.25±0.08	0.25±0.06
Gastrointestinal tract[c]	1.6±0.2	2±1	0.86±0.07
Carcass[d]	18±5	6.2±0.9	5±1

[a]Each data point presents an average from 4 animals ± SD and is expressed as the percent of injected radioactivity per gram organ or tissue. Data are the mean ± SD (n=4). [b]A small piece of colon (100-150 mg) was dissected and the uptake was measured; [c]radioactivity was presented as % IA in the whole gastrointestinal tract with content, except for a small 100- to 150-mg piece of colon. [d]The radioactivity in the carcass was presented as % IA.

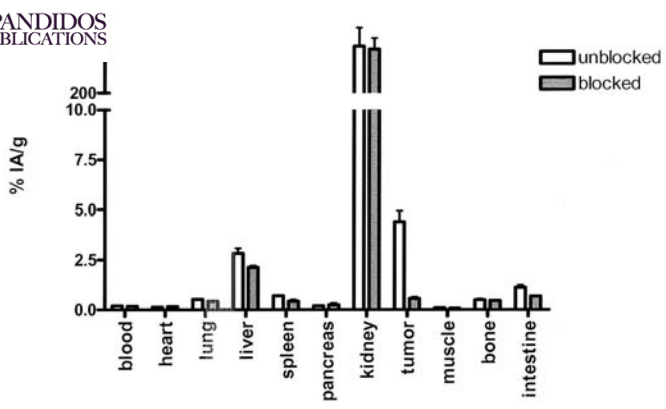

Figure 2. Specificity of ^{111}In-benzyl-DOTA-$Z_{HER2:342}$ uptake *in vivo* 4 h pi (mice bearing LS174T xenografts). One group of animals (blocked) was pre-injected with 475 μg $Z_{HER2:342}$ to saturate HER2 receptors 1 h before injection of radiolabeled conjugate. All animals were injected with 1 μg ^{111}In-benzyl-DOTA-$Z_{HER2:342}$. Data are the mean ± SD (n=4).

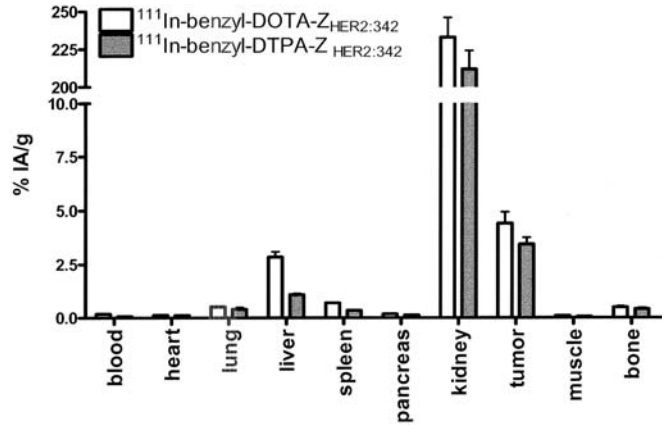

Figure 3. Comparison of the biodistribution of ^{111}In-benzyl-DOTA-$Z_{HER2:342}$ and ^{111}In-benzyl-DTPA-$Z_{HER2:342}$ in nude mice bearing LS174T xenografts 4 h pi. All animals were injected with ~1 μg of radiolabeled conjugate. Data are the mean ± SD (n=4).

For this reason, it is difficult to interpret the results of the internalization test.

Biodistribution studies. A study in normal mice was performed to assess blood and whole body clearance and to identify organs with high uptake of radioactivity. The results are presented in Table I. The conjugate was characterized by quick blood clearance, with 1.1±0.2% IA/g 1 h pi and 0.21±0.04% IA/g 4 h pi. The accumulation of radioactivity in a majority of organs was correlated to the radioactivity concentration in the blood. The radioactivity in the gastrointestinal tract was low, indicating that the hepatobiliary excretion plays a minor role. At the same time, the radioactivity accumulation in the liver had no tendency to decrease throughout the study, indicating that internalization of the residualizing indium-111 label occurred. Still, this accumulation was rather low, < 2% IA/g. The organ with the highest radioactivity accumulation was the kidney. Already at 1 h pi, 44±3% of the injected radioactivity (146±31% IA/g) was accumulated in the kidneys, and there was no significant

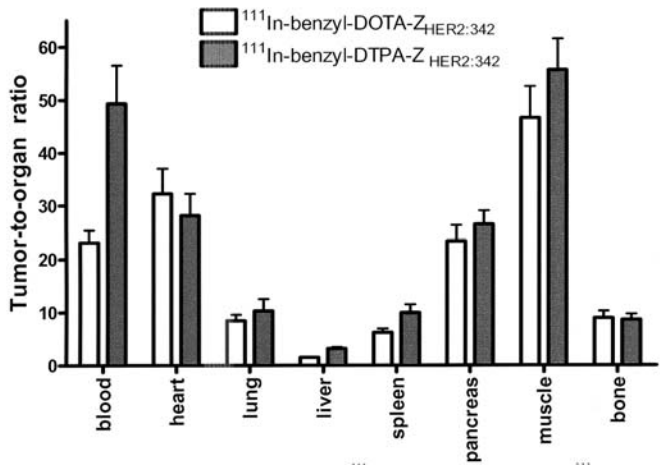

Figure 4. Tumor-to-organ ratio 4 h after injection of ^{111}In-benzyl-DOTA-$Z_{HER2:342}$ and ^{111}In-benzyl-DTPA-$Z_{HER2:342}$ in nude mice bearing LS174T xenografts. Data are the mean ± SD (n=4).

reduction of kidney radioactivity during the observation period. The radioactivity concentration in the bone was low and constant between 4 and 24 h pi.

The biodistribution of ^{111}In-benzyl-DOTA-$Z_{HER2:342}$ in nude mice bearing LS174T xenografts is presented in Fig. 2 as well as the effect of a pre-injection of a large amount of non-labeled $Z_{HER2:342}$. Although the HER2 expression in LS174T colon carcinoma cells was rather low, the radioactivity concentration in the tumor (4.4±1.0% IA/g) exceeded the uptake in all organs and tissues, except for the kidneys (232±25% IA/g). The pre-injection of a large amount of non-labeled $Z_{HER2:342}$ reduced the tumor uptake 7.7-fold, to 0.6±0.2% IA/g ($p<0.0005$). The blocking of the tumor uptake indicates its saturability and confirms its receptor-mediated nature. Besides tumors, uptake was significantly ($p<0.05$) reduced in the lungs, liver and spleen. The magnitude of this reduction was 1.2-1.6 times smaller than the reduction in the tumors.

A comparison of the biodistribution of ^{111}In-benzyl-DOTA-$Z_{HER2:342}$ and ^{111}In-benzyl-DTPA-$Z_{HER2:342}$ is presented in Fig. 3. The general pattern of biodistribution was similar for both conjugates, with quick blood clearance, high renal uptake and a tumor uptake exceeding the uptake in normal organs, except the kidneys. The difference between the radioactivity accumulation in the kidneys and the tumors was not statistically significant. However, there was a significant ($p<0.01$) difference between the accumulation of these two conjugates in the blood, liver, spleen, pancreas, and muscles, where the radioactivity concentration at 4 h after injection of ^{111}In-benzyl-DOTA-$Z_{HER2:342}$ was 1.5-2.5 times higher than after injection of ^{111}In-benzyl-DTPA-$Z_{HER2:342}$. A significant difference ($p<0.05$) in tumor-to-organ ratios was found only for the blood and the liver (Fig. 4). At this point of time, the tumor-to-blood ratios were 23±5 and 50±14, and the tumor-to-liver ratio was 1.5±0.1 and 3.2±0.6 for ^{111}In-benzyl-DOTA-$Z_{HER2:342}$ and ^{111}In-benzyl-DTPA-$Z_{HER2:342}$, respectively.

γ-camera imaging. Images acquired 4 h after the administration of the ^{111}In-benzyl-DOTA-$Z_{HER2:342}$ to immuno-

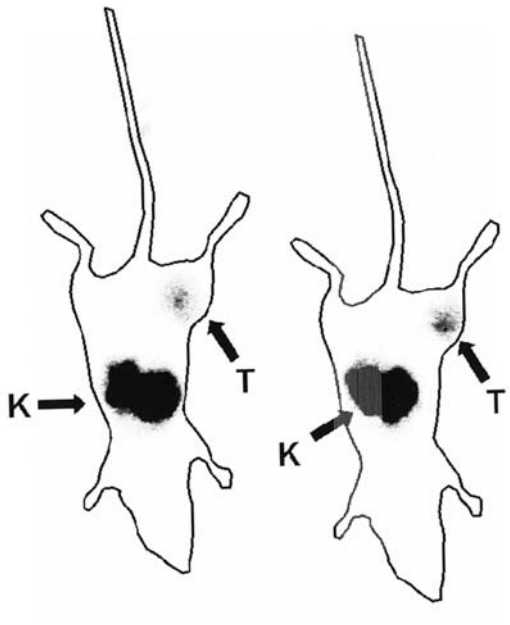

Figure 5. Planar γ-camera imaging of HER2 expression in SKOV-3 xenografts in Balb/c nude mice using ^{111}In-benzyl-DOTA-$Z_{HER2:342}$ (4 h pi). Tumors (hind legs) were clearly visualized. Schematic animal outlines are superimposed over images to facilitate interpretation. Arrows indicate the positions of the kidneys (K) or tumors (T).

deficient mice bearing subcutaneous SKOV-3 tumors revealed a high tumor localization of the radioactivity (Fig. 5). As predicted from the biodistribution studies described above, the renal route of elimination of the conjugates also led to substantial kidney retention. Tumor-to-non-tumor ratios were (average ± maximum error) 33±7 for contralateral thigh, 0.21±0.01 for the kidneys, and 3.3±0.1 for the liver. The higher tumor-to-non-tumor ratios found in the imaging experiment in comparison to the biodistribution data could be explained by using SKOV-3 xenografts with higher HER2 expression than LS174T.

Discussion

The development of labeling methods for scaffold proteins is a challenging problem. With their size and complexity of structure, Affibody molecules occupy an intermediate position between small peptides and antibody fragments. The labeling chemistry of both these groups has been studied relatively well. In small peptides, a pendant group which is necessary for the attachment of a radionuclide, constitutes an appreciable part of the conjugate and often influences its binding capacity and biodistribution dramatically. At the same time, peptides often allow for rather harsh labeling and purification conditions, such as high temperatures, extreme pH, and the use of lipophilic solvents, which would denature antibodies (34). The biodistribution and binding properties of antibodies are relatively insensitive to the nature of a pendant group, if the antibody is not overmodified, but sensitive to labeling conditions. The influence of labeling methods on targeting properties of scaffold protein-based targeting agents needs to be studied further before we will be able to implement them in nuclear molecular imaging.

The DOTA chelator provides a very stable labeling with ^{111}In, $^{68/67}$Ga, and ^{86}Y due to the kinetical inertness of the chelates. The same inertness necessitates the use of elevated temperatures for chelation, and the literature often reports on labeling at 80-100˚C using long reaction times (28,35,36). In our case, >95% labeling efficiency was obtained within 5 min at a lower temperature, 60˚C. The difference is not easily understood, but might well be due to the fact that the work with robust short peptides did not force other researchers to reduce the labeling time and decrease the labeling temperature. Another explanation might be that the good labeling results were ensured by strict metal-free routines in our laboratory (purification of all buffers by Chelex resin and acid washes of vials). Improvement of DOTA labeling by meticulous implementation of metal-free techniques was observed by other researchers as well (37). Moreover, quick labeling at modest temperatures might be explained by the use of ammonium acetate as a buffer. According to the observation of Professor Maecke, the use of ammonium and acetate in buffers provides better results than the use of sodium and citrate (Professor H.R. Maecke, private communication). The results of the EDTA challenge indicate that true DOTA chelation was obtained. Blocking experiments demonstrated that the labeled ^{111}In-benzyl-DOTA-$Z_{HER2:342}$ conjugate preserved its capacity for specific binding to HER2-expressing cells *in vitro* and targeting of HER2-expressing xenografts *in vivo* (Fig. 2). The reduction of radioactivity uptake in the lungs, liver and spleen after injection of a blocking amount of non-labeled $Z_{HER2:342}$ (Fig. 2) indicates that there might be cross-reactivity of $Z_{HER2:342}$ with the murine counterpart of HER2, which correlates well with our previous observations concerning ^{111}In-benzyl-DTPA-$Z_{HER2:342}$ (26). Still, both unspecific and specific uptake in normal tissues was rather low, which provided a good tumor-to-organ ratio even in the case of LS174T xenografts with low HER2 expression (Fig. 4).

Direct comparison with ^{111}In-benzyl-DTPA-$Z_{HER2:342}$ (Fig. 3) showed that the use of benzyl-DOTA instead of benzyl-DTPA influenced the overall biodistribution of ^{111}In-labeled $Z_{HER2:342}$. Though the blood clearance remained quick for the benzyl-DOTA conjugate, the radioactivity concentration in the blood was ~2.6 times higher than for the acyclic chelator. The same ratio was found between concentrations of radioactivity in the liver. It is difficult to distinguish between the cause and effect. Both the lower glomerular filtration rate and the larger distribution volume in the liver of ^{111}In-benzyl-DOTA-$Z_{HER2:342}$ might have caused the observed biodistribution. Although ^{111}In-benzyl-DOTA-$Z_{HER2:342}$ gave an elevated radioactivity concentration in the spleen, pancreas and muscle, only the tumor-to-blood and the tumor-to-liver ratios were significantly lower for this conjugate. Despite the lower affinity, the tumor uptake of ^{111}In-benzyl-DOTA-$Z_{HER2:342}$ did not differ significantly from the uptake of ^{111}In-benzyl-DTPA-$Z_{HER2:342}$. It should be noted that the affinity of the benzyl-DOTA conjugate was still in the subnanomolar range. The radioactivity concentration in bone did not differ between these conjugates, though DTPA is considered a weaker chelator. The blood residence time of the Affibody-DTPA conjugate might be too short to be seriously

d by the circulating transferrin. Taken together, a demonstrated that even for a relatively small scaffold protein, such as the Affibody molecule (the molecular weight with the chelator is ~8 kDa), the chelator can influence the biodistribution of the conjugate, and such an influence should be evaluated.

It should be noted that although the tumor-to-non-tumor ratio of ^{111}In-benzyl-DOTA-$Z_{HER2:342}$ was lower than that of ^{111}In-benzyl-DTPA-$Z_{HER2:342}$, it was still well suitable for *in vivo* imaging, as demonstrated by the γ-camera experiment. The SKOV-3 ovarian carcinoma cell line, which was used for the development of xenografts in the imaging study, expresses about 1.2 million HER2s per cell (38), which matches tumors with 3+ expression of HER2. Such xenografts can be visualized with high contrast. The radioactivity accumulation in the liver was lower than that in the tumor, as seen in Fig. 5.

The only organ, which had a higher radioactivity accumulation than the tumor, was the kidney. This might complicate imaging of targets located close to the kidneys. On the other hand, the kidney could be well located using SPECT/CT or (with an appropriate nuclide) PET/CT, which excludes misinterpretation of images. For this reason, we do not consider high renal uptake as a serious problem for the introduction of DOTA-$Z_{HER2:342}$ into clinical practice.

In conclusion, isothiocyanate-benzyl-DOTA was coupled to the anti-HER2 Affibody molecule $Z_{HER2:342}$. The obtained conjugate was efficiently labeled with ^{111}In in relatively mild conditions and preserved its capacity to bind selectively to HER2-expressing cells. ^{111}In-benzyl-DOTA-$Z_{HER2:342}$ demonstrated a capacity to specifically target HER2-expressing xenografts *in vivo*, though providing lower contrast than ^{111}In-benzyl-DTPA-$Z_{HER2:342}$. The results of this study open a path for the investigation of benzyl-DOTA-$Z_{HER2:342}$ conjugates labeled with positron-emitting radiometals (^{68}Ga, ^{55}Co and ^{86}Y) and with radiolanthanides for locoregional therapy.

Acknowledgements

This study was financially supported by grants from the Swedish Cancer Society (Cancerfonden) and the Swedish Research Council (VR). We thank Veronika Eriksson and the animal facility staff of the Rudbeck laboratory for the technical assistance. We thank Dr Joachim Feldwisch, Dr Anders Wennborg and Dr Lars Abrahmsén (Affibody AB) for their interesting and inspiring discussions on the use of Affibody molecules for imaging and comments on the manuscript.

References

1. Yarden Y and Sliwkowski MX: Untangling the ErbB signalling network. Nat Rev Mol Cell Biol 2: 127-137, 2001.
2. Carlsson J, Nordgren H, Sjostrom J, *et al*: HER2 expression in breast cancer primary tumours and corresponding metastases. Original data and literature review. Br J Cancer 90: 2344-2348, 2004.
3. Meden H and Kuhn W: Overexpression of the oncogene c-erbB-2 (HER2/neu) in ovarian cancer: a new prognostic factor. Eur J Obstet Gynecol Reprod Biol 71: 173-179, 1997.
4. Wester K, Sjöström A, de la Torre M, Carlsson J and Malmström PU: HER-2 - a possible target for therapy of metastatic urinary bladder carcinoma. Acta Oncol 41: 282-288, 2002.
5. Baselga J, Norton L, Albanell J, Kim YM and Mendelsohn J: Recombinant humanized anti-HER2 antibody (Herceptin) enhances the antitumor activity of paclitaxel and doxorubicin against HER2/neu overexpressing human breast cancer xenografts. Cancer Res 58: 2825-2831, 1998.
6. Adams CW, Allison DE, Flagella K, *et al*: Humanization of a recombinant monoclonal antibody to produce a therapeutic HER dimerization inhibitor, pertuzumab. Cancer Immunol Immunother 55: 717-727, 2006.
7. Neckers L: Hsp90 inhibitors as novel cancer chemotherapeutic agents. Trends Mol Med 8 (suppl 4): 55-61, 2002.
8. Yeon CH and Pegram MD: Anti-erbB-2 antibody trastuzumab in the treatment of HER2-amplified breast cancer. Invest New Drugs 23: 391-409, 2005.
9. Wolff AC, Hammond ME, Schwartz JN, *et al*: American Society of Clinical Oncology/College of American Pathologists guideline recommendations for human growth factor receptor 2 testing in breast cancer. J Clin Oncol 25: 118-145, 2007.
10. Molina R, Barak V, van Dalen A, *et al*: Tumor markers in breast cancer - European Group on Tumor Markers recommendations. Tumour Biol 26: 281-293, 2005.
11. Smith-Jones PM, Solit DB, Akhurst T, Afroze F, Rosen N and Larson SM: Imaging the pharmacodynamics of HER2 degradation in response to Hsp90 inhibitors. Nat Biotechnol 22: 701-706, 2004.
12. Zidan J, Dashkovsky I, Stayerman C, Basher W, Cozacov C and Hadary A: Comparison of HER-2 overexpression in primary breast cancer and metastatic sites and its effect on biological targeting therapy of metastatic disease. Br J Cancer 93: 552-556, 2005.
13. Behr TM, Behe M and Wormann B: Trastuzumab and breast cancer. N Engl J Med 345: 995-996, 2001.
14. Perik PJ, Lub-De Hooge MN, Gietema JA, *et al*: Indium-111-labeled trastuzumab scintigraphy in patients with human epidermal growth factor receptor 2-positive metastatic breast cancer. J Clin Oncol 24: 2276-2282, 2006.
15. Smith-Jones PM, Solit D, Afroze F, Rosen N and Larson SM: Early tumor response to Hsp90 therapy using HER2 PET: Comparison with 18F-FDG PET. J Nucl Med 47: 793-796, 2006.
16. Tang Y, Wanga J, Scollarda DA, Mondala H, Holloway C, Kahn HJ and Reilly RM: Imaging of HER2/neu-positive BT-474 human breast cancer xenografts in athymic mice using ^{111}In-trastuzumab (Herceptin) Fab fragments. Nucl Med Biol 32: 51-58, 2005.
17. Deyev SM, Waibel R, Lebedenko EM, Schubiger AP and Pluckthun A: Design of multivalent complexes using the barnase barstar module. Nat Biotechnol 21: 1486-1492, 2004.
18. Hey T, Fiedler E, Rudolph R and Fiedler M: Artificial, non-antibody binding proteins for pharmaceutical and industrial applications. Trends Biotechnol 23: 514-522, 2005.
19. Nord K, Gunneriusson E, Ringdahl J, Ståhl S, Uhlén M and Nygren PA: Binding proteins selected from combinatorial libraries of an alpha-helical bacterial receptor domain. Nat Biotechnol 15: 772-777, 1997.
20. Wikman M, Steffen AC, Gunneriusson E, Tolmachev V, Adams GP, Carlsson J and Ståhl S: Selection and characterisation of HER2/neu-binding affibody ligands. Protein Eng Des Sel 17: 455-462, 2004.
21. Steffen AC, Wikman M, Tolmachev V, Adams GP, Nilsson F, Ståhl S and Carlsson J: *In vitro* characterization of a bivalent anti-HER-2 affibody with potential for radionuclide based diagnostics. Cancer Biother Radiopharm 20: 239-248, 2005.
22. Mume E, Orlova A, Nilsson F, Larsson B, Nilsson AS, Sjöberg S and Tolmachev V: Evaluation of (4-hydroxyphenyl)ethyl) maleimide for site-specific radiobromination of anti-HER2 affibody. Bioconjug Chem 16: 1547-1555, 2005.
23. Orlova A, Nilsson F, Wikman M, Ståhl S, Carlsson J and Tolmachev V: Comparative *in vivo* evaluation of iodine and technetium labels on anti-HER2 affibody for single-photon imaging of HER2 expression in tumors. J Nucl Med 47: 512-519, 2006.
24. Steffen AC, Orlova A, Wikman M, *et al*: Affibody mediated tumor targeting of HER-2 expressing xenografts in mice. Eur J Nucl Med Mol Imaging 33: 631-638, 2006.
25. Orlova A, Magnusson M, Eriksson T, *et al*: Tumor imaging using a picomolar affinity HER2 binding Affibody molecule. Cancer Res 66: 4339-4348, 2006.
26. Tolmachev V, Nilsson FY, Widström C, Andersson K, Gedda L, Wennborg A and Orlova A: ^{111}In-benzyl-DTPA-$Z_{HER2:342}$, an Affibody-based conjugate for *in vivo* imaging of HER2 expression in malignant tumors. J Nucl Med 47: 846-853, 2006.

27. Breeman WAP, de Jong M, Visser TJ, Erion JL and Krenning EP: Optimising conditions for radiolabelling of DOTA-peptides with ^{90}Y, ^{111}In and ^{177}Lu at high specific activities. Eur J Nucl Med Mol Imaging 30: 917-920, 2003.
28. Onthank DC, Liu S, Silva PJ, Barrett JA, Harris TD, Robinson SP and Edwards DS: ^{90}Y and ^{111}In complexes of a DOTA-conjugated integrin alpha v beta 3 receptor antagonist: different but biologically equivalent. Bioconjug Chem 15: 235-241, 2004.
29. Olafsen T, Kenanova VE, Sundaresan G, *et al*: Optimizing radiolabeled engineered anti-p185HER2 antibody fragments for *in vivo* imaging. Cancer Res 65: 5907-5916, 2005.
30. Liu S and Edwards DS: Bifunctional chelators for target specific therapeutic lanthanide radiopharmaceuticals. Bioconjug Chem 12: 7-34, 2001.
31. Tolmachev V, Orlova A, Wei Q, Bruskin A, Carlsson J and Gedda L: Comparative biodistribution of potential anti-glioblastoma conjugates [^{111}In]DTPA-hEGF and [^{111}In]Bz-DTPA-hEGF in normal mice. Cancer Biother Radiopharm 19: 491-501, 2004.
32. Milenic DE, Garmestani K, Brady ED, Albert PS, Ma D, Abdulla A and Brechbiel MW: Targeting of HER2 antigen for the treatment of disseminated peritoneal disease. Clin Cancer Res 10: 7834-7841, 2004.
33. Milenic DE, Garmestani K, Brady ED, Albert PS, Ma D, Abdulla A and Brechbiel MW: α-Particle radioimmunotherapy of disseminated peritoneal disease using a ^{212}Pb-labeled radioimmunoconjugate targeting HER2. Cancer Biother Radiopharm 20: 557-568, 2005.
34. Lundqvist H and Tolmachev V: Targeting peptides and positron emission tomography. Biopolymers 66: 381-392, 2002.
35. Giblin MF, Gali H, Sieckman GL, Owen NK, Hoffman TJ, Forte LR and Volkert WA: *In vitro* and *in vivo* comparison of human *Escherichia coli* heat-stable peptide analogues incorporating the ^{111}In-DOTA group and distinct linker moieties. Bioconjug Chem 15: 872-880, 2004.
36. Storch D, Behe M, Walter MA, Chen J, Powell P, Mikolajczak R and Macke HR: Evaluation of [^{99m}Tc/EDDA/HYNIC0] octreotide derivatives compared with [^{111}In-DOTA0,Tyr3,Thr8] octreotide and [^{111}In-DTPA0]octreotide: does tumor or pancreas uptake correlate with the rate of internalization? J Nucl Med 46: 1561-1569, 2005.
37. Hainsworth JE and Mather SJ: Regressive DOTA labelling performance with indium-111 and yttrium-90 over a week of use. Eur J Nucl Med Mol Imaging 32: 1348, 2005.
38. Persson M, Tolmachev V, Andersson K, Gedda L, Sandström M and Carlsson J: [^{177}Lu]pertuzumab. Experimental studies on targeting of HER-2 positive tumour cells. Eur J Nucl Med Mol Imaging 32: 1457-1462, 2005.